

## HIGH INTENSITY BEAM PHYSICS AT UMER

B. L. Beaudoin, S. Bernal, M. Cornacchia, K. Fiuza, I. Haber, R.A. Kishek, T.W. Koeth, M. Reiser, D.F. Sutter, H. Zhang, and P.G. O’Shea, Institute for Research in Electronics and Applied Physics, University of Maryland, College Park, MD 20742, U.S.A.

### Abstract

We report on progress of studies of transverse and longitudinal space-charge beam physics at the University of Maryland electron ring (UMER), a low-energy, high current recirculator. The transverse beam dynamics studies include measurements of betatron and dispersion functions as well as linear resonances for a number of beam currents. We also discuss the implementation of induction focusing for the longitudinal containment of the lowest current beam. When complemented with optimized orbit steering, this longitudinal beam focusing has made possible to extend the number of turns from 100 to more than 1,000, limited mostly by electronics. Some of the results presented are compared with calculations and simulations with the computer codes ELEGANT and WARP.

In one case (0.6 mA), we have the additional capability of longitudinal confinement of the beam through inductively-produced voltage pulses applied at the bunch ends. As discussed below, longitudinal focusing dramatically increases the transport distance. Additional details of this topic can be found in Ref. [3].

The paper is organized as follows: in the first two sections we present results of transverse beam dynamics (lattice functions and linear resonances); in the third section we summarize the implementation of longitudinal focusing for the low current beam, including a brief discussion of a simple 1D model and space charge waves, and in the last section we present the summary and conclusions.

### INTRODUCTION

The University of Maryland Electron Ring (UMER) is a high intensity circular machine that is dedicated to the study of long path length space-charge dominated beam and accelerator physics on a small scale [1]. Understanding how space-charge modifies beam transport from the “zero current” linear optics theory to a regime of highly depressed tune is of fundamental interest to transporting high current bright beams for long distances.

Table 1 summarizes the parameters of the beams currently under study in UMER. The values in the last two columns result from calculations in a uniform focusing model [1]. All beams have pulse duration close to 100 ns, with a 60 Hz repetition rate. Further, the beams are injected with a single-turn scheme involving a fast magnetic kicker and 2 wide-aperture magnetic quadrupoles [2]. The diagnostics employed consist of 14 fast capacitive beam position monitors (BPMs) located every 64 cm around the 11.52 m-circumference ring except for three locations that are fitted with glass breaks. At one of these locations, roughly half way around the ring and labelled “RC10”, a fast wall current monitor is employed to measure the AC component of the circulating beam current.

### LATTICE FUNCTIONS

The techniques employed for measuring betatron and dispersion functions in UMER are standard [4], but the space-charge tune depressions at injection are not (see Table 1).

We use quadrupole-current scans to determine the betatron function, and energy scans to calculate the dispersion function. The following well-known approximation [4], as applied to UMER, relates the betatron function at a given quadrupole to the changes in coherent tune ( $\Delta\nu$ ) and quadrupole strength ( $\Delta k \propto \Delta I_{Quad}$ ) when the latter is sufficiently small:

$$\beta_{x,y} [cm] = \pm 317 \frac{\Delta V_{x,y}}{\Delta I_{Quad} [A]}. \quad (1)$$

We obtain  $\beta_x = 13.7 \pm 4.6$  cm,  $\beta_y = 18.2 \pm 1.9$  cm from a quadrupole scan near halfway around the ring at the standard operating point (ring quadrupole current equal to 1.819 A) for the 6.0 mA beam. Calculations with the code Elegant [5] yield  $\beta_x = 23.9$  cm,  $\beta_y = 41.3$  cm. Betatron beating from mismatch is most likely the reason for the differences, with a small contribution (not included in Elegant) from defocusing by image forces.

With 72 quadrupoles in UMER, measuring the betatron function is clearly tedious, even more so if this has to be repeated for all beam currents. Thus, other techniques like those based on the response matrix are being explored. But other questions arise when applying standard techniques to beams with high space-charge. For example, if we consider Eq. (1), it could be assumed that to first order there is no change in the contribution to focusing from space charge as the external focusing is varied. In addition, the contribution from linear space-charge to the tune variation (numerator in Eq. (1)) would

Table 1: Parameters of 3 Electron Beams in UMER at 10 keV and Nominal Operating Bare Tune of 6.6

Beam Current	Norm. RMS Emittance	Av. Beam Radius	Tune Depression
0.6 mA	$0.4 \pm 20\%$ $\mu\text{m}$	1.6 mm	0.86
6.0	$1.3 \pm 10\%$	3.4	0.63
21	$1.5 \pm 10\%$	5.2	0.31

cancel out. Therefore, we would end up with the same zero-current betatron function. In a real situation, however, the beam may be so mismatched from a small change in external focusing that the contribution from space-charge also changes; in this case, there would be no straightforward way to determine  $\Delta v/\Delta k$ . Further, a simple analysis shows that linear space charge leads to a larger, *current-dependent* betatron function equal to the zero-current one divided by the tune depression. Therefore, unless special beam diagnostics are implemented to detect incoherent tune, standard techniques based on beam position monitors alone would only yield the “undepressed” betatron function. In any case, the information provided by this function for different beam currents is of interest for testing the ideas just presented as well as for machine characterization.

We have also measured the dispersion function for the 0.6 mA and 6.0 mA beams at the locations of the 14 BPMs around the ring. Figure 1 below shows preliminary results of horizontal dispersion for the two beam currents at an operating ring quadrupole current of 1.840 A ( $\nu_0 = 6.70$ ), slightly higher than the standard.

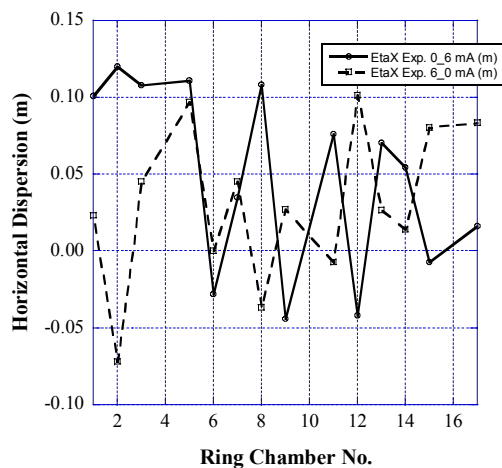


Figure 1: Measured horizontal dispersion in UMER for 0.6 mA (solid line) and 6.0 mA (dashed line) beams at 10 keV. The nominal bare tune is close to 6.70.

From Fig. 1 data, the average dispersions for the 0.6 mA, 6.0 mA cases are 4.9 cm, 3.1 cm, respectively. The calculated average zero-current dispersion at the same operating point is  $\rho/\nu_0^2 = 4.1$  cm ( $\rho = 1.83$  m, average bending radius). The differences between the two dispersion functions in Fig. 1 can be qualitatively understood by 1) the different conditions of the wide-aperture quadrupoles at injection, 2) the resulting differences in degrees of mismatch of the dispersion function, and 3) measurement errors (larger for 0.6 mA). Calculations with the code ELEGANT, on the other hand, show only fair agreement with measurements; the average dispersion in the ELEGANT calculation is 5.8 cm.

As for the betatron function, there are questions about the validity of the standard techniques for dispersion function measurements when space-charge is significant.

Since the BPMs in UMER are currently sensitive to beam dipole moment alone, the only effect from space charge forces that can be detected is from image forces. Thus, to measure the effect of incoherent space charge forces on dispersion, second moments of the beam distribution would have to be determined and supplemented with measurements of energy spread of the beam. For a given uncorrelated energy spread, the theories developed independently some years ago by Venturini-Reiser and Lee-Okamoto [6] for continuous beams predict a larger average dispersion for larger space charge intensities, but not as large as  $\rho/\nu^2$ , where  $\nu$  is the depressed tune.

## LINEAR BETATRON RESONANCES

We have extended the resonance studies reported in Ref. [7] to include 2-dimensional tune scans for 0.6, 6.0 and 21 mA beams at 10 keV. As before, we measure the transmitted current at a given turn (typically the 5th, 10th, and 20th turns) over a broad range of quadrupole strengths. For the new studies, the currents of both focusing and defocusing quadrupoles are varied from 1.65 to 2.09 A in steps of 10 mA, keeping the same matching solution for the rms-envelope throughout, i.e., the solution employed at the default operating point (quadrupole current of 1.819 A, or bare tune  $\nu_0 = 6.56$ ). In addition, we measure the tune at 10-12 points of good current transmission and fit a model calculation in order to generate a simple algorithm to translate all quadrupole current pairs into bare tunes. The simplest model for tune calculations involves a ring lattice of identical quadrupoles with an effective quadrupole gradient strength of 3.84 G/cmA. The model yields good agreement with horizontal tune measurements but systematic lower tunes for the vertical plane; this is in agreement with the expected contribution of image forces. Initial identification of resonances is possible with the simple model, but refined calculations are underway involving more realistic magnets and image force effects. In Figure 2 we present examples of tune charts of transmitted-current for the 0.6 and 6.0 mA beams.

We observe strong integer resonances within 5-10 turns, particularly in the vertical plane,  $\nu_{0Y} = 6.0, 7.0$ , for all beams. Half-integer resonances,  $\nu_{0Y} = 6.5, 7.5$ , appear early for the low-current beam mostly in the vertical plane and develop gradually for 6.0 mA. There is also a sum (coupling) resonance that develops for the 6.0 mA beam and is clearly seen at the 20th turn (not shown in Fig. 2.)

As expected, the integer resonances are very strong and their early appearance is in agreement with calculations employing standard single-particle theory and reasonable assumptions for dipole strength and quadrupole transverse displacement errors in UMER [8]. The only noticeable difference between the beams is the wider stopband at  $\nu_{0Y} = 7.0$  for the pencil beam. The half-integer resonances, on the other hand, are seen for 0.6 mA and 6.0 mA at bare tunes close to the expected values in both horizontal and vertical planes, except for  $\nu_{0Y} = 6.5$  near the standard operating point.

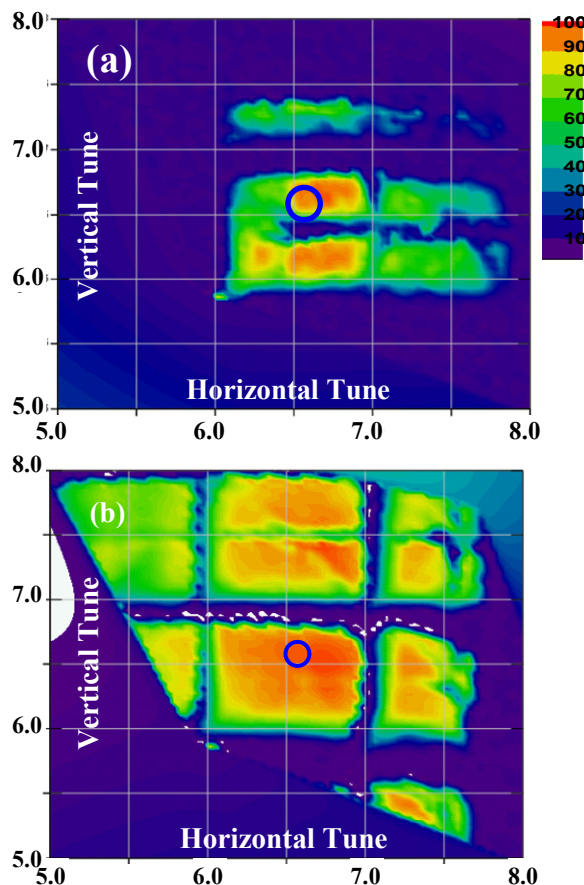


Figure 2: Fractional transmitted current as a function of bare tunes at the 10<sup>th</sup> turn for two beams: (a) 0.6 mA, and (b) 6.0 mA. Linear resonance bands are clearly seen. The blue circle indicates the standard operating tunes at 10 keV.

When space charge plays a significant role, resonances are properly understood in terms of frequencies of collective beam modes and the harmonics of the lattice error spectrum. As an example, the conditions for excitation of a quadrupole mode are approximately satisfied for the 0.6, 6.0 and 21 mA beams in the neighbourhood of a bare tune  $\nu_0 = 6.20$ , but with different modes being excited (envelope tunes of 11, 9 and 7 for 0.6, 6.0 and 21 mA, respectively.) In principle, a single quadrupole gradient error such as from one of the wide-aperture quadrupoles in the UMER injector could excite all envelope modes. However, we do not have evidence so far of such mode excitation, from a single gradient error or otherwise. Several factors can explain this: emittance may be rapidly evolving such that mode excitation does not have time to develop, or any modes that are excited are quickly damped by collective mechanisms involving nonlinear space charge and other factors from, e.g., longitudinal beam dynamics. In addition, although the equations used to calculate envelope tunes are valid for arbitrarily large tune shift, they also assume small mismatch and a K-V beam distribution; these last two conditions are generally not satisfied in UMER. Finally, although tunes can be

understood as RMS-equivalent quantities for non-uniform beam distributions, there are also anisotropies in emittance and focusing as well as possible effects from transverse-longitudinal coupling.

At this stage in our studies, better understanding of envelope and dispersion matching and beam losses is perhaps more important for unravelling the complicated situation of resonances in UMER than invoking refined models of mode excitation.

## LONGITUDINAL CONFINEMENT

Another important aspect to consider for improved beam transport particularly with high intensity beams is the effect of space charge on the longitudinal beam dynamics.

Under the influence of longitudinal space charge forces the beam ends expand until the front of the bunch overtakes the rear of the bunch, filling the ring with charge. Then, the ability to resolve peak currents per turn using the AC coupled diagnostic is lost and an apparent current loss is detected as the beam becomes DC. The lifetime of the 0.6 mA (peak current) beam is approximately 25  $\mu\text{s}$  (i.e. 125 turns) with no confinement. This is illustrated in Figure 3 below.

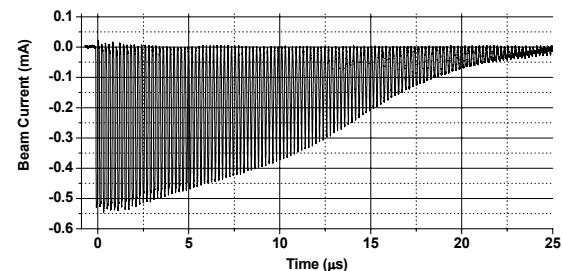


Figure 3: Beam current measured at the RC10 wall current monitor without the application of longitudinal focusing. The signal is baseline restored using a circuit solver.

Induction focusing is employed to contain the bunch longitudinally via synchronized periodically-applied electric fields. Figure 4 illustrates the focusing synchronization at a rate of one application for every 5 turns or 1013.1996 kHz.

When longitudinal confinement is applied to the beam, the beam ends are unable to overtake each other. This assists in maintaining the AC structure of the beam; the resulting signal from the RC10 wall current monitor is shown in Figure 5. With the longitudinal confinement, the beam lifetime is extended by a factor of ten or beyond 200  $\mu\text{s}$  (greater than 11.52 km) [3].

The axial fields necessary to contain the beam bunch can be calculated using a model for longitudinal end-erosion that represents the beam as a 1-D fluid. In this model, the beam is assumed to be a cylinder of charge with radius  $R$ , line-density  $\lambda$  and beam velocity  $v$  (so beam current is  $I = \lambda v$ ) inside a pipe of radius  $b$ .

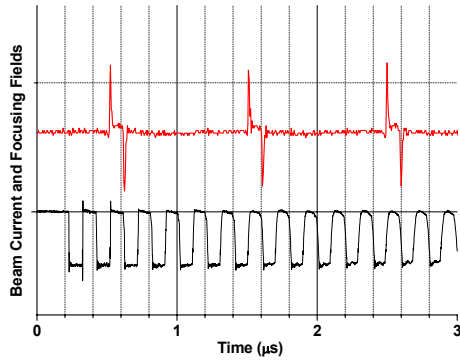


Figure 4: Axial focusing field burst pattern for the 0.6 mA beam. The bottom curve represents the beam revolving at 5.066 MHz measured at the current monitor, and the top curve represents the confinement fields applied once every five revolutions or 1013.1996 kHz. Vertical axes are in arbitrary units.

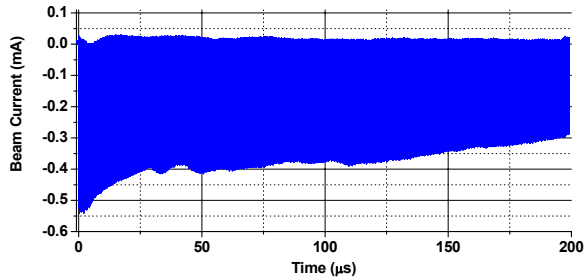


Figure 5: Beam current measured at the RC10 wall current monitor with longitudinal focusing applied every five beam revolutions.

The phase velocity of space charge waves in the beam frame is the sound speed given by

$$C_s = \sqrt{\frac{q}{\gamma_0^5 m} \frac{g}{4\pi\epsilon_0}} \lambda_0, \quad (2)$$

where  $q$  is the electron charge,  $m$  the electron mass,  $\gamma_0$  the Lorentz factor,  $\epsilon_0$  the permittivity of free space and the variable  $g = 2 \ln(b/R)$  is the geometry factor. This factor accounts for the beam pipe shielding of the longitudinal electric fields [1]. Assuming that a bunch with constant line-density and velocity is injected into the ring, the longitudinal electric fields in the central region of the bunch will be equal to zero (from the derivative of the line-density [1].) However, gradients in the line-density near the bunch-ends lead to longitudinal electric self-fields that push particles in the bunch ends away from the central region, causing the bunch to expand longitudinally at a rate of  $2C_s$  [9-13]. This is also accompanied by a rarefaction of

the ends which erode into the bunch at a rate of  $C_s$ . Particles at the head are accelerated forward while particles in the tail are accelerated backwards from the main bunch, within the beam frame. By solving the one-dimensional fluid equations, we can obtain line-density and velocity analytical wave solutions describing the current and velocity profiles as they evolve [9, 12]. Table 2 summarizes results of sound speed [Eq. (2)] and the number of turns that the bunch ends take before they meet. The initial bunch's duration is 100 ns.

Table 2: Sound Speeds from Eq. (2) and Number of Turns for Bunch Ends to Meet

Beam Current	Sound Speed $C_s$	No. of Turns for ends to meet
0.6 mA	$2.9 \times 10^5$ m/s	25
6.0	$8.0 \times 10^5$	9
21	$13.8 \times 10^5$	5

Figure 6 shows the evolution of the beam's bunch over 100 turns without longitudinal containment. It takes about 25 turns for the bunch ends to meet.

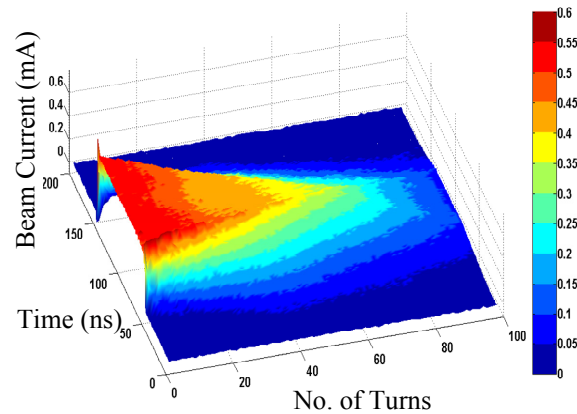


Figure 6: Evolution over 100 turns of an initially 100 ns square beam pulse for the 0.6 mA (initial peak current) beam.

As already mentioned, the expansion of the head and tail can be counteracted through the periodic application of axial electric fields with the appropriate parameters to re-establish and preserve the rectangular beam current profile over a long distance (see Fig. 5). However, proper synchronization and frequency of the axial fields is required to optimize the longitudinal containment and minimize the appearance of space charge waves inside the bunch. An example of the latter is shown in Fig. 7 below.

Similar longitudinal focusing is necessary to extend the propagation distance of the high current beams in UMER. These beams would require an application of stronger and more frequent axial fields. The improved transport of

these beams should prove crucial for additional studies of both longitudinal and transverse dynamics.

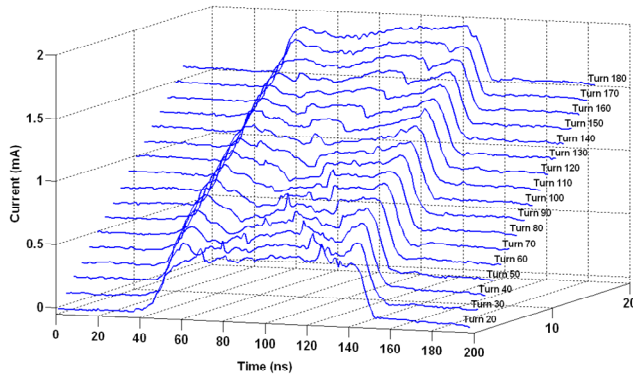


Figure 7: Evolution over 180 turns of space charge waves induced by mismatch of longitudinal focusing of the 0.6 mA (peak current) beam.

## SUMMARY AND CONCLUSIONS

We have presented results of studies on both transverse and longitudinal beam dynamics in UMER. We have discussed our preliminary measurements of betatron and dispersion functions as a function of beam current and shown that measurements based on beam centroid can only yield “undepressed” quantities. Further, we have described our observations of linear resonances for low and high current; beam losses and longitudinal expansion, particularly for high current, limit the number of turns we can achieve, but clear differences in the stopbands of the low and high current beams is detected nonetheless.

We have also presented successful results on the longitudinal confinement of a low current electron beam. This achievement has given us the capability of extending beam transport by at least a factor of 10, allowing us to study long path-length space-charge dominated physics in a small scale ring.

We are still in the process of understanding the mechanisms responsible for beam losses within the first few hundred turns and how mismatch of the applied confinement fields at the edges of the bunch induce space-charge waves within the bunch. This understanding will help us to extend longitudinal focusing to higher current beams.

## ACKNOWLEDGMENTS

This work was supported by the U.S. Department of Energy Office of Fusion Energy Science and Office of High Energy Physics, and by the Department of Defense Office of Naval Research and Joint Technology Office.

## REFERENCES

[1] M. Reiser, Theory and Design of Charged Particle Beams 2<sup>nd</sup> Ed., Wiley-VCH Inc, 2008.

[2] Hui Li, "Control and Transport of Intense Electron Beams", Ph.D. Thesis, University of Maryland, College Park, 2004.

[3] B.L. Beaudoin, S. Bernal, I. Haber, R.A. Kishek, T. Koeth, D. Sutter, and P.G. O'Shea, "Longitudinal Confinement of an Intense Beam Using Induction Focusing," Proceedings of 14th Workshop on Advanced Accelerator Concepts (AAC), Annapolis, MD, June 2010, (New York: AIP Press, 2010).

[4] F. Zimmermann, "Precise Accelerator Models Using Measurements with Beam", Proceedings of EPAC 2000, Vienna, Austria, p. 141.

[5] M. Borland, "Elegant: A Flexible SDDS-Compliant Code for Accelerator Simulation", Advanced Photon Source LS-287, September 2000.

[6] M. Venturini and M. Reiser, "rms Envelope Equations in the Presence of Space Charge and Dispersion", Phys. Rev. Lett. 81, 1, 96 (1998); S. Y. Lee and H. Okamoto, "Space-Charge Dominated Beams in Synchrotrons", Phys. Rev. Lett. 80, 23, 5133 (1998).

[7] S. Bernal, B. Beaudoin, T. Koeth, M. Cornacchia, D. Sutter, K. Fiuza, I. Haber, R.A. Kishek, C. Wu, C. Papadopoulos, M. Reiser, and P.G. O'Shea, "Resonance Phenomena Over a Broad Range of Beam Intensities in an Electron Storage Ring" in Proceedings of PAC09, Vancouver, Canada, (to be published).

[8] S. Bernal, "Simple Calculations for Integer Resonance Crossing and Applications to UMER", UMER Technical Note UMER-090915-SB, Sep. 2009 (unpublished).

[9] D. Wang, Ph.D. Dissertation, University of Maryland, 1993, pp.142.

[10] A. Friedman, J.J. Barnard, R.H. Cohen, D.P. Grote, S.M. Lund, W.M. Sharp, A. Faltens, E. Henestroza, J-Y. Jung, J.W. Kwan, E.P. Lee, M.A. Leitner, B.G. Logan, J.-L. Vay, W.L. Waldron, R.C. Davidson, M. Dorf, E.P. Gilson, I. Kaganovich, Proc. International Computational Accelerator Physics Conference (ICAP) 09, San Francisco, CA, 2009.

[11] B. Beaudoin, Master Thesis, University of Maryland, 2008, pp.37.

[12] A. Faltens, E.P. Lee, and S.S. Rosenblum, J. Appl. Phys. 61 (12), 15 June 1987, pp.5219.

[13] B. Beaudoin, S. Bernal, K. Fiuza, I. Haber, R.A. Kishek, P.G. O'Shea, M. Reiser, D. Sutter, and J.C.T. Thangaraj, "Longitudinal Beam Bucket Studies for a Space-Charge Dominated Beam," Proceedings of the 2009 IEEE Particle Accelerator Conference, Vancouver, BC, Paper ID, FR5FPF058 (2009).